

Subtraction Gets You More: Gap-Aware Retrieval for Multimodal Multi-Hop QA

Sunah O Jay-Yoon Lee *
Seoul National University
{ec_osa16586, lee.jayyoon}@snu.ac.kr

Abstract

In multimodal multi-hop question answering, we focus on the initial retrieval stage via two distinct tasks: (1) evidence set completion, retrieving missing evidence given context, and (2) sequential pool construction, iteratively building the top- K pool from the scratch. Under these settings, we point out that conventional iterative retrieval frameworks often suffer from Semantic Anchoring, where previously fetched evidence traps the retriever and yields entity-centric redundancy. To break this trap, we propose **GRAIL** (Gap-aware Retrieval via Adaptive Implicit Localization), a paradigm that performs implicit query rewriting directly at the embedding level. By context-subtractive query steering, GRAIL excels at compositional cross-modal reasoning, while additive embedding updates show strength on localized information aggregation. By dynamically routing queries based on task type, our Hybrid Framework achieves a **40.3%** macro-averaged performance gain on MultimodalQA. Extensive evaluations demonstrate that sequential GRAIL retrieves in a superior, noise-resilient manner, significantly expanding the search horizon through iterative gap-aware optimization.

1 Introduction

In multimodal retrieval-augmented generation frameworks, the reasoning performance of Large Multimodal Models (LMMs) is fundamentally contingent on the quality of the evidence pool. While text-only tasks often allow models to rely on broad parametric knowledge, multimodal multi-hop questions answering (MMQA) demands a direct inspection of explicit, modality-specific details. Without having these context-dependent facts provided, LMMs cannot infer the high-density visual or structural details—such as specific trends in a chart or the color of objects—that are crucial for accurate reasoning. Consequently, retrieval is not merely a

preliminary step; it effectively sets the performance ceiling of the entire retrieval-augmented LMM.

To address multi-step dependencies, a single, initial query is inherently insufficient to cover the entire sequence of required evidence. A straightforward alternative is to decompose the complex question a priori into independent sub-queries and execute them sequentially (Talmor et al., 2021). Yet, such static decomposition frameworks immediately founder when confronted with open-domain multimodality. In a vast multimodal corpus, it is nearly impossible to predict which modality—whether text, image, or table—contains the specific piece of evidence required for each hop. Because the modality of target facts remain unknown before the search begins, pre-determining a rigid textual decomposition pathway is structurally unviable.

To overcome this predictability barrier, a more dynamic paradigm has emerged: given an initial subset of evidence, subsequent queries are iteratively regenerated by adding the acquired context. However, as illustrated in Figure 1, this evidence-additive query regeneration loop exhibits a critical structural failure we define as Semantic Anchoring. Instead of expanding the search space, the strong semantic gravity of previously fetched evidence traps the retriever, forcing an over-reliance on prominent entities (e.g., Lancashire Senior Cup). This leads to entity-centric redundancy, blindly fetching redundant assets while pushing the true target evidence—the *complementary fact regarding Bolton’s emblem*—out of the top- K rank.

One might also ask why not simply rely on advanced LMMs for explicit query regeneration. In practice, forcing dense visual observations through a narrow textual detour introduces non-trivial token overhead and a high susceptibility to semantic drift. When an explicit text-generation agent prematurely commits to an incorrect textual path—such as anchoring heavily on *Manchester City* (Figure 1)—the trajectory error compounds catastrophically. The

*Correspondence author

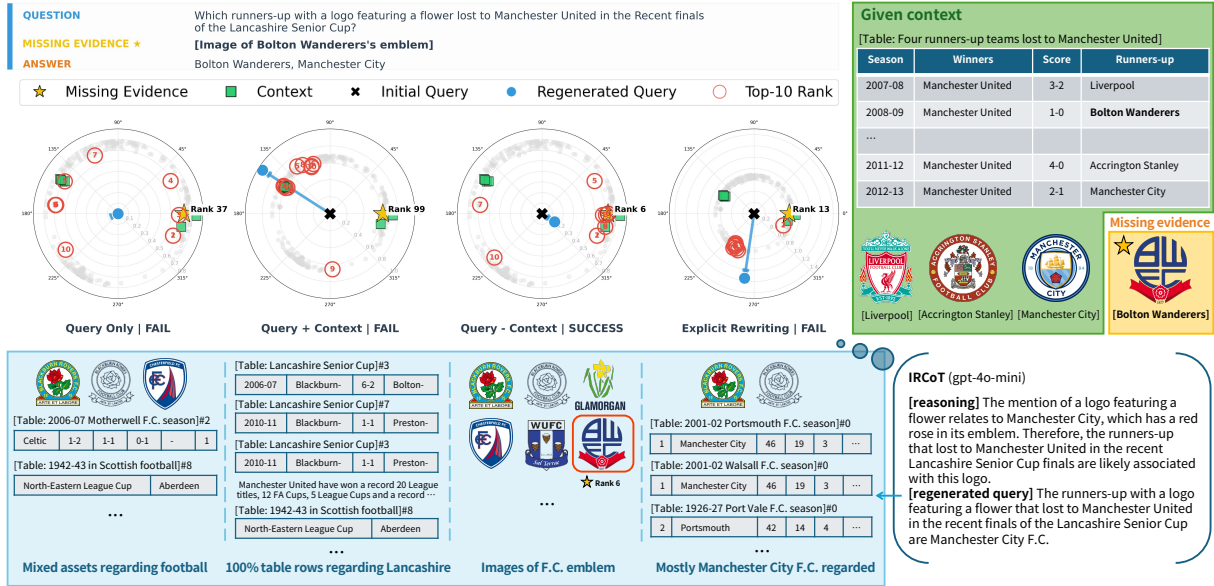


Figure 1: **Redundancy trap in MMQA.** Given a table and three emblems, the goal is to fetch the missing visual evidence (*Bolton Wanderers's emblem*) to complete the evidence set. (i) Query + Context fail as they trapped by the existing *Lancashire Senior Cup* context (Semantic Anchoring). Meanwhile, Explicit Rewriting (IRCoT) prematurely concludes the search upon verifying *Manchester City's* record, overlooking the unexamined visual assets. (ii) Query – Context succeeds by implicitly subtracting the covered context features within the embedding space, shifting the search direction toward the unobserved visual target. See Appendix A for another case study.

language-centric bias misdirects subsequent search iterations toward redundant or irrelevant spaces, proving that explicit textification fails to capture unexamined, complementary multi-modal assets.

We introduce **GRAIL** (Gap-aware Retrieval via Adaptive Implicit Localization), a new paradigm for implicit query rewriting within the latent space. Rather than blindly contextualizing existing context, the rewritten query consistently shifts toward the unanswered facets of the question, increasing its similarity to missing evidence by subtracting the already covered information from the query. Operating entirely in the embedding space, this mechanism avoids any linguistic loss and enables an efficient, self-correcting retrieval trajectory for complex MMQA. When applied iteratively, it naturally supports progressive evidence discovery without accumulating semantic bias.

The primary contributions are as follows:

- **Problem Identification:** We systematically characterize Semantic Anchoring in MMQA, demonstrating how conventional iterative loops suffer from entity-centric redundancy (Figure 1).
- **Implicit Latent Steering:** We propose **GRAIL** that performs context-subtractive query rewriting directly in the latent space, mitigating semantic anchoring in additive retrieval.

- **Task-Adaptive Hybrid Framework:** Based on a comparative analysis of where gap-aware versus additive search excels, we design a hybrid framework that dynamically routes queries to handle both evidence aggregation and missing evidence retrieval.
- **Robust Iterative Retrieval:** When applied iteratively on multimodal evidence, our mechanism constructs high-quality Top- K candidate pools; unlike conventional additive methods prone to compounding errors, **GRAIL** remains robust to noise and prevents error propagation.

2 Related Work

Multimodal Question Answering Early works in MMQA primarily focus on downstream reasoning or query decomposition under heavily constrained, "closed-world" environments. Frameworks such as AutoRouting (Talmor et al., 2021), ImplicitDecomp (Talmor et al., 2021), PREasM (Yoran et al., 2022), SKURG (Yang et al., 2023), and RAMQA (Bai et al., 2025) inherently rely on pre-filtered asset pools provided by the dataset metadata, without executing open-domain candidate retrieval. Even within these oracle-guided pools, PREasM (Yoran et al., 2022) restricts its reasoning scope to text and table only, while RAMQA

(Bai et al., 2025) is limited to single-hop QA. Furthermore, although MuRAG (Chen et al., 2022) scales to full-wiki image-text corpora, it lacks iterative reasoning across heterogeneous modalities. While existing networks excel at localized reasoning under distractor settings, they do not explicitly address the challenges of open-domain, multimodal, multi-hop retrieval. More recently, frameworks like LILaC (Yun et al., 2025) have introduced explicit LLM-based query decomposition coupled with structural graph traversal. However, since discrete planning systems are vulnerable to cascading planning errors, we execute implicit query steering directly within the embedding space.

Multi-hop Retrieval Within the text-only domain, iterative retrieval and query reformulation—such as recursive vector addition in MDR (Xiong et al., 2021), explicit entity expansion in GoldEn (Qi et al., 2019), or LLM-based generation in IR-CoT (Trivedi et al., 2023) and IterDRAG (Yue et al., 2025)—have widely pioneered sequential context construction. However, translating text-centric paradigms into multimodal contexts introduces severe bottlenecks. Explicit textification of high-dimensional visual features is computationally expensive, flattens non-verbal cues into rigid keywords, and triggers compounding hallucinations or semantic drift.

Space Purification We introduce subtractive query steering, conceptually rooted in Rocchio relevance feedback (Rocchio, 1971) and its dense retrieval extensions via contrastive learning and hard negative mining (Karpukhin et al., 2020; Xiong et al., 2020; Izacard et al., 2021). While conventional multi-hop methods refine queries through the additive accumulation of retrieved evidence (Xiong et al., 2021), our framework executes online, implicit subtraction to dynamically suppress redundant context and prevent semantic drift. Importantly, unlike classic Rocchio feedback, it eliminates explicit centroid updates or static weighting, learning to purify the multimodal latent space via a differentiable, step-wise gated transformation.

3 Problem Formulation

3.1 Evidence Set Completion

Multimodal multi-hop question answering (MMQA) requires integrating multiple pieces of evidence across diverse modalities to derive a concise answer. In an open-domain setting, this

process necessitates retrieving a set of relevant items from a vast, multi-modal corpus \mathcal{C} . While previous studies often focus on the downstream reasoning stage, we shift our attention exclusively to the retrieval phase: the fundamental process of gathering the necessary information to enable such multi-hop reasoning.

Let q be a query representation and $\mathcal{E}^* = \{e_1, e_2, \dots, e_G\}$ be the gold evidence set required to resolve q . Assuming a partial evidence subset $\mathcal{E}_p \subset \mathcal{E}^*$ has already been acquired, the retriever’s objective is to identify the missing evidence piece $e_t \in \mathcal{E}^* \setminus \mathcal{E}_p$ from \mathcal{C} . Unlike standard retrieval paradigms that optimize for individual asset relevance in isolation, evidence set completion demands a complementary optimization of the candidate pool. The primary goal is to learn a mapping function $f(q, \mathcal{E}_p) \rightarrow q'$ that generates a gap-aware, reformulated query, which adaptively suppresses the information components already covered by \mathcal{E}_p .

3.2 Sequential Pool Construction

A practical open-domain MMQA scenario does not provide any partial gold context a priori. Therefore, we extend the single-step completion into a sequential retrieval task, where the retriever must autonomously construct set of evidences \mathcal{E}_{ret} ($|\mathcal{E}_{\text{ret}}| = K$) starting from a query-only state ($\mathcal{E}_p = \emptyset$).

At the initial hop $t = 0$, the retriever dispatches q to fetch an initial chunk of base evidence $\mathcal{E}_{\text{base}}$ of size A ($< K$) from the corpus \mathcal{C} . The partial evidence set is initialized with this base context, establishing $\mathcal{E}_p^{(0)} = \mathcal{E}_{\text{base}}$. At each subsequent hop $t \in \{1, 2, \dots, T\}$, the mapping function processes the original query along with the accumulated context to formulate an updated retrieval vector:

$$q^{(t)} = f(q, \mathcal{E}_p^{(t-1)}). \quad (1)$$

This vector is deployed to retrieve a complementary block of evidence $\mathcal{B}^{(t)}$ of size $M^{(t)}$. The acquired context is then dynamically expanded via set union:

$$\mathcal{E}_p^{(t)} = \mathcal{E}_p^{(t-1)} \cup \mathcal{B}^{(t)}. \quad (2)$$

The iterative process terminates when the total accumulated evidence fulfills the remaining slots ($\sum_{t=1}^T M^{(t)} = K - A$), yielding the final integrated candidate pool $\mathcal{E}_{\text{ret}} = \mathcal{E}_p^{(T)}$.

As the refinement hops proceed, the trajectory of $q^{(t)}$ must continuously escape the semantic gravity of $\mathcal{E}_p^{(t-1)}$ to discover novel information gaps, thereby maximizing the density of valid evidence within a limited candidate budget K .

4 Methodology

While our framework executes implicit trajectory steering within a shared latent space, managing this embedding topology reveals foundational structural anomalies.

First, multi-hop search paths suffer from **Entity-Centric Bias**, where dominant entities within the initial query q overwhelm the embedding space, fetching redundant assets with diminishing returns (see Figure 1). While breaking this trap necessitates a transition from additive to a subtractive query reformulation, executing such latent feature purification introduces a secondary bottleneck: the **Invisible Modality Gap**. Because semantic redundancy often transcends modalities, where information in one format (e.g., a film script) may offer the same utility as another (e.g., a corresponding video frame), a disjointed embedding space prevents the retriever from detecting covered information. Consequently, precise cross-modal alignment is a strict prerequisite for effective feature subtraction.

To resolve these limitations, GRAIL operates in two sequential stages: (1) **Unified Semantic Alignment (4.1)** synchronizes multimodal vector topologies into a consistent embedding space to enable cross-format redundancy evaluation. (2) **Gap-aware Search Mechanism (4.2)** balances acquiring novel complementary information with preserving the original query relevance, suppressing redundant context features from \mathcal{E}_p while maintaining the required logical reasoning path for q .

4.1 Unified Semantic Alignment

The first stage establishes a unified semantic space of text, tables, and images. This alignment is a functional prerequisite for the subsequent bi-encoder retrieval, ensuring that evidence from any modality can be compared and operated upon within a consistent vector space.

Alignment Strategies We evaluate four strategies, categorized into two query-independent and two query-dependent options.

Query-independent alignments focus on the internal cohesion of the evidence set \mathcal{E}^* : (a) *Centroid-based* minimizes the distance between the mean vector of \mathcal{E}^* and its members, while (b) *CLS-based* utilizes the hidden state of the [CLS] token from the concatenated sequence $[[CLS]; e_1; \dots; e_G]$ as a semantic anchor. Conversely, query-dependent approaches incorporate query information into

the alignment process: (c) *Query-evidence* explicitly maps q to each individual $e_i \in \mathcal{E}^*$, whereas (d) *Query-set* processes the joint sequence $[q; e_1; \dots; e_G]$ to utilize the query token’s final hidden state as the alignment pivot.

These alignment strategies differ only in their definition of the anchor representation. For a batch of size N , let anc_x be the designated anchor embeddings for x -th sample. We optimize an InfoNCE loss to maximize the semantic agreement between this anchor-evidence pairs:

$$\mathcal{L}_{\text{align}} = -\frac{1}{N} \sum_{x=1}^N \frac{1}{|\mathcal{E}_x^*|} \sum_{e \in \mathcal{E}_x^*} \log \frac{\mathcal{P}^x(e)}{\mathcal{P}^x(e) + \mathcal{N}^x} \quad (3)$$

where $\mathcal{P}^x(e)$ and \mathcal{N}_x denote the intra-chain positive alignment score and inter-chain negative contrastive score, respectively:

$$\mathcal{P}^x(e) = \exp(\text{sim}(anc_x, e)/\tau) \quad (4)$$

$$\mathcal{N}^x = \sum_{y \neq x}^N \sum_{e' \in \mathcal{E}_y^*} \exp(\text{sim}(anc_x, e')/\tau) \quad (5)$$

where τ is the temperature parameter and $\text{sim}(\cdot, \cdot)$ denotes the similarity function (e.g., cosine similarity).

By switching the formulation of anc , this objective scales across all strategies introduced above. For example, query-evidence strategy (c) simply instantiates the anchor as $anc_x = q_x$. This unified formalization provides the multi-modal space with the exact topological precision required before executing the subsequent information subtraction stage.

4.2 Gap-aware Search Mechanism

Upon the unified latent space, we build a search mechanism to identify the information gap. Overall process is summarized in Algorithm 1.

Information Aggregation To represent the knowledge already acquired from \mathcal{E}_p , compute an existing knowledge vector h_{ctx} :

$$h_{\text{ctx}} = \text{LN} \left(\sum_{e_i \in \mathcal{E}_p} \alpha_i e_i \right) \quad (6)$$

where the attention weight α_i is defined as:

$$\alpha_i = \frac{\exp((e_i \cdot q)/\sqrt{d})}{\sum_{e_j \in \mathcal{E}_p} \exp((e_j \cdot q)/\sqrt{d})} \quad (7)$$

where d is the dimension of the shared latent space.

Context-Subspace Removal To isolate the missing information, we generate the updated query intent via an implicit context-subtractive rewriting of q relative to h_{ctx} . Unlike the unconstrained trajectory expansion of conventional additive search ($q + h_{\text{ctx}}$), our learnable gap gate $g = \sigma(W_{\text{gap}}[q; h_{\text{ctx}}])$ dynamically modulates the steering intensity based on the accumulated context:

$$q_{\text{gap}} = q - g \cdot \left(\frac{q \cdot h_{\text{ctx}}}{\|h_{\text{ctx}}\|^2} \right) h_{\text{ctx}} \quad (8)$$

where $W_{\text{gap}} \in \mathbb{R}^{1 \times 2d}$ and q_{gap} represents the purified query intent for missing evidence. By design, g uniformly scales the overlapping context to mitigate semantic redundancy without distorting the embedding topology.

The final retrieval vector h_{req} is constructed by dynamically mixing q_{gap} and h_{ctx} :

$$h_{\text{req}} = \text{LN}(w_1 q_{\text{gap}} + w_2 h_{\text{ctx}}) \quad (9)$$

where the adaptive weights $[w_1, w_2]$ are computed as $\text{Softmax}(W_{\text{mix}}[q_{\text{gap}}; h_{\text{ctx}}])$ with $W_{\text{mix}} \in \mathbb{R}^{2 \times 2d}$.

End-to-End Joint Optimization All components are optimized jointly and end-to-end without any auxiliary losses or separate heuristics. Because every operation in the gap-aware search mechanism is fully differentiable, the retrieval success signal directly backpropagates to steer these parameters. Specifically, given a training batch of size N , let h_{req}^x be the dynamically steered request vector for the x -th query sample, and e_t^x be its corresponding desired evidence. The model is optimized using the multiple negatives ranking loss formulated as:

$$\mathcal{L}_{\text{InfoNCE}} = -\frac{1}{N} \sum_{x=1}^N \log \frac{\mathcal{P}_{\text{ncc}}^x(e_t^x)}{\mathcal{P}_{\text{ncc}}^x(e_t^x) + \mathcal{N}_{\text{ncc}}^x} \quad (10)$$

where $\mathcal{P}_{\text{ncc}}^x(e_t^x)$ and $\mathcal{N}_{\text{ncc}}^x$ denote the positive retrieval score and the negative contrastive score for the x -th sample, respectively:

$$\mathcal{P}_{\text{ncc}}^x(e) = \exp(\text{sim}(h_{\text{req}}^x, e) / \tau_{\text{dyn}}^x) \quad (11)$$

$$\mathcal{N}_{\text{ncc}}^x = \underbrace{\sum_{y \neq x}^N \mathcal{P}_{\text{ncc}}^x(e_t^y)}_{\text{In-batch negatives}} + \underbrace{\sum_{z \in \mathcal{Z}^x} \mathcal{P}_{\text{ncc}}^x(z)}_{\text{Hard distractors}} \quad (12)$$

where \mathcal{Z}^x represents the set of hard multimodal distractors. The retrieval score is calibrated using a dynamic temperature τ_{dyn}^x , which automatically regulates how aggressively the network learns from each context.

4.3 Task-Adaptive Hybrid Framework

The optimal strategy for retrieval fundamentally diverges across different question categories. For example, certain queries benefit from additive reinforcement ($h_{\text{req}}^{\text{add}}$) to consolidate ongoing context, while others strictly demand subtractive query steering ($h_{\text{req}}^{\text{gap}}$) to isolate missing information. To exploit these distinct operational advantages, we introduce a *Task-Adaptive Hybrid Framework* governed by a front-end query selector. By analyzing the incoming query q , a lightweight selector $\Phi(q) \in \{0, 1\}$ pre-determines the most effective specialist framework before executing the document search:

$$h_{\text{req}} = \begin{cases} h_{\text{req}}^{\text{add}}, & \text{if } \Phi(q) = 0 \\ h_{\text{req}}^{\text{gap}}, & \text{if } \Phi(q) = 1 \end{cases} \quad (13)$$

The selector $\Phi(q)$ is a Transformer-based sequence encoder topped with a linear classification layer. Independent of the retrieval training, the selector is optimized using a standard cross-entropy loss on a labeled subset $\mathcal{D}_{\text{route}} = \{(q, \text{label})\}$, where ground-truth labels are automatically mapped based on task metadata (i.e., $y = 0$ for information aggregation tasks, and $y = 1$ for specific target isolation tasks). Once trained to distinguish reasoning topologies, the selector parameters are frozen. During inference, this gate acts as a deterministic paradigm switch, structurally enabling task-specialized synergy.

5 Experiments

5.1 Experimental Setup

5.1.1 Dataset

We utilize the **MultimodalQA** benchmark (Talmor et al., 2021); its corpus and dataset statistics are detailed in Appendix B.1 (Table 4 and Table 5). (See Appendix F for WebQA dataset evaluation.)

To evaluate the model’s ability to identify the information gap, we reformulate the original MultimodalQA into the Evidence Set Completion task. Based on the gold evidence sets \mathcal{E}^* , we filter for instances where $|\mathcal{E}^*| \geq 2$. Specifically, we expand each question-evidence set pair into multiple test instances by iteratively withholding each evidence item $e_i \in \mathcal{E}^*$ as the **missing evidence** ($e_t = e_i$) while providing all other items in the set as the **context** ($\mathcal{E}_p = \mathcal{E}^* \setminus \{e_t\}$). This exhaustive leave-one-out approach ensures that the model is evaluated on its ability to retrieve any missing component e_t from the full corpus \mathcal{C} regardless of the provided context.

5.1.2 Baselines

Unless specified otherwise, all models are evaluated under the *Query-evidence* alignment (see Appendix B.3 for full implementation details). We compare GRAIL against several competitive alternatives, ranging from standard dense retrieval to large language model (LLM) query regeneration:

- **Query Only:** A standard dense bi-encoder (DPR-style (Karpukhin et al., 2020)) that retrieves evidence solely relying on the original query q .
- **Additive:** The search vector is updated by adding the query and context embeddings, analogous to PRF / Rocchio-style relevance feedback (Rocchio, 1971) in dense retrieval (see Algorithm 1).
- **LLM-based Query Regeneration:** We adapt text-based multi-hop methods to multimodal settings using gpt-4o-mini (Hurst et al., 2024):
 - **Closed-Book Generation:** The LLM regenerates a search query based solely on q , evaluating the baseline performance of internal parametric knowledge.
 - **IRCoT:** Adapted from IRCoT (Trivedi et al., 2023), the LLM generates a reasoning trace given q and \mathcal{E}_p , where visual assets are fed as raw images.
 - **Answer-Augmented Retrieval:** The LLM generates an intermediate answer from the context, which is then concatenated to the query ($\text{ans} \oplus q$).

5.1.3 Evaluation Metrics

To evaluate retrieval quality and dissect the inner mechanics, we use two primary performance metrics and three diagnostic metrics.

Primary Performance Metrics For Evidence Set Completion (3.1), we utilize **Recall@K**, measuring whether the single missing target evidence e_t is retrieved. ($\text{R@K} = \mathbb{I}(\text{rank}(e_t) \leq K)$.) For Sequential Pool Construction (3.2), we employ **Set-Recall@K** to quantify the coverage of the candidate pool \mathcal{E}_{ret} against the gold evidence set \mathcal{E}^* :

$$\text{Set-Rec@K}(\mathcal{E}_{\text{ret}}) = \frac{|\mathcal{E}_{\text{ret}} \cap \mathcal{E}^*|}{|\mathcal{E}^*|}. \quad (14)$$

Diagnostic Metrics First, to quantify the semantic trajectory of retrieval vectors and empirically diagnose the phenomenon of semantic anchoring, we introduce the **Semantic Escape Delta** (Δ_{esc}):

$$\Delta_{\text{esc}} = \text{sim}(q', e_t) - \max_{e_i \in \mathcal{E}_p} \text{sim}(q', e_i). \quad (15)$$

A positive Δ_{esc} indicates that the steered query vector has successfully broken out of the semantic gravity of the satisfied context \mathcal{E}_p toward the unexplored logical void of the missing target e_t .

Second, to evaluate the framework’s capability to maximize the information density of the limited candidate pool, we introduce the **Rank Jump** (*Jump*). Formally, let \mathcal{E}_{q_0} denote the top- K evidences retrieved solely by the raw query q (corresponding to the $\mathcal{E}_{\text{base}}$ size of K). The subset of newly included target assets \mathcal{S} is formulated as:

$$\mathcal{S} = (\mathcal{E}_{\text{ret}} \cap \mathcal{E}^*) \setminus \mathcal{E}_{q_0} \quad (16)$$

The Rank Jump for a given query q is computed as the mean baseline rank of these elevated assets:

$$\text{Jump}(q) = \frac{1}{|\mathcal{S}|} \sum_{e_i \in \mathcal{S}} \text{rank}_{q_0}(e_i) \quad (17)$$

where $\text{rank}_{q_0}(e_i)$ represents the initial rank of asset e_i under the Query Only retrieval. A higher *Jump* score empirically demonstrates that the model effectively surfaces informative, low-ranked assets into the top- K slots, thereby constructing a highly efficient, information-dense candidate pool.

Third, to quantify the self-purifying capacity under adversarial initial states, we introduce the **Noise-Resilience Margin** (*NRM*). We isolate a subset of highly challenging queries, \mathcal{Q}_n , where $\mathcal{E}_{\text{base}}$ contains absolutely zero gold items ($\mathcal{E}_{\text{base}} \cap \mathcal{E}^* = \emptyset$). For this 100% noisy subset, *NRM* measures the net recall gain achieved by the retrieval model over the Query Only alternative:

$$\text{NRM} = \frac{1}{|\mathcal{Q}_n|} \sum_{q \in \mathcal{Q}_n} (\text{Set-Rec@K}(\mathcal{E}_{\text{ret}}) - \text{Set-Rec@K}(\mathcal{E}_{q_0})) \quad (18)$$

A positive *NRM* confirms model’s self-correcting capability; the model successfully limits error propagation and prevents the query from veering off in meaning, navigating back to the target assets even when starting from a completely noisy context.

5.2 Specialization: Anchoring vs. Purification

Divergent Performance Patterns Table 1 and Figure 2 reveal a clear functional decoupling: Additive integration excels in *Uni-modal* and *Intersect* tasks by acting as a “topic reinforcer” within localized semantic domains, but fails significantly in *Compare* and *Compose* tasks requiring entity transitions or cross-modal leaps (see Appendix C.2 for further analysis). In these reasoning-heavy settings, the Additive model suffers from **semantic anchoring**, where the context locks the search vector and

Table 1: **Evidence Set Completion performance across question types in MultimodalQA.** While the additive baseline performs well on localized aggregated tasks (*Uni-modal*, *Intersect*), GRAIL achieves clear gains on compositional reasoning tasks (*Compose*, *Compare*), additionally supported by the positive Δ_{esc} .

Type	Method	R@1	R@5	R@10	R@20	Δ_{esc}
Uni-	Additive	37.67	61.00	70.38	77.84	-0.139
	GRAIL	21.00	33.94	40.91	46.72	-0.010
Intersect	Additive	23.00	45.71	52.81	61.90	-0.111
	GRAIL	14.61	30.70	38.10	46.50	-0.066
Compare	Additive	4.28	12.59	16.63	24.47	-0.245
	GRAIL	18.29	33.25	38.72	45.84	+0.046
Compose	Additive	7.44	19.38	26.90	33.10	-0.292
	GRAIL	20.31	36.51	42.79	50.00	+0.087

blocks the transition to distinct targets. Conversely, GRAIL dominates these tasks, outperforming the baseline by up to threefold (20.31% vs. 7.44% in *Compose*).

Overcoming Semantic Gravity As shown in Table 1, the Additive model’s Δ_{esc} consistently drops into negative values, indicating that the query representation is swallowed by the semantic gravity of the satisfied context. Mathematically, simple addition cannot generate a search signal orthogonal to what is already retrieved. Conversely, GRAIL executes successful **semantic purification**, maintaining a positive escape margin (+0.087 in *Compose*). By subtracting redundant projections, it creates a repelling force that drives the retrieval vector into the remaining information gap.

The Hybrid Framework This task-specific specialization highlights the necessity of a hybrid

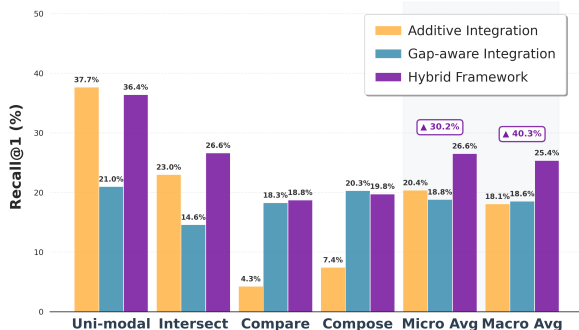


Figure 2: **Hybrid framework leveraging complementary specialists in MultimodalQA.** By dynamically routing each query to the optimal specialist, our hybrid framework achieves a "best-of-both-worlds" performance (+40.3% macro avg. gain over Additive).

Table 2: **Implicit vs. Explicit query modeling performance and latency.** We evaluated macro-averaged recall across the MultimodalQA validation split (2,724 data, $q_type \in \{\text{Compare, Compose, Intersect}\}$). Our GRAIL & Hybrid consistently outperform both the additive baseline and explicit query regeneration baselines.

Method	R@1	R@3	R@5	R@10	Latency
Query Only	16.24	32.68	<u>40.51</u>	48.54	2–5 ms
<i>Explicit Query Generation</i>					
Closed-Book	13.78	26.89	34.65	42.69	0.6–1.0 s
IRCoT	13.42	24.87	30.18	36.21	1.1–1.6 s
Ans-Augmented	16.54	33.24	39.96	<u>48.86</u>	1.2–1.8 s
<i>Implicit Vector Steering</i>					
Additive	11.57	25.89	32.11	39.82	2–5 ms
GRAIL	<u>17.74</u>	<u>33.49</u>	39.87	47.45	3–6 ms
Hybrid (ours)	20.53	38.49	44.77	52.58	3–6 ms

framework that routes queries based on reasoning requirements. We train two distinct specialist—each optimized exclusively for their respective top-performing question type—and integrate them via a learned query router, which achieves an accuracy of 97.71% (F1-score: 0.98) on the validation split. Consequently, this dynamic assignment yields a **+6.2pp gain** in micro average R@1 (Figure 2).

5.3 Effectiveness of Implicit Query Steering

Table 2 compares our implicit update models with explicit baselines relying on LLM-generated text queries. While methods like IRCoT attempt to trace human-like reasoning, they suffer from a linguistic bottleneck. In multimodal settings, translating high-dimensional visual features into discrete text tokens triggers semantic loss; rich, non-verbal cues are compressed into a few keywords, failing to capture the subtle relational information. Furthermore, the poor performance of Closed-Book and IRCoT—even fall behind the Query Only baseline—demonstrates that explicit text generation can act as a **semantic distractor**. Inaccurate textual synthesis misdirects the search agent, proving that implicit vector steering directly within the embedding space is fundamentally more robust than error-prone textual translations (see Figure 1 and Appendix A for qualitative case studies).

5.4 Achieving Extended Effective Top-K

To evaluate practical efficiency in a realistic pipeline, we analyze sequential pool construction strategies where the evidence pool is built from scratch without relying on oracle context. Table 3

Table 3: **Granular efficiency under various step configurations** ($K = 10$). Performance changes are relative to the Query Only baseline; Jump values are reported as mean (90th percentile). Results demonstrate that sequential GRAIL outperforms both static additive interpolation and single-shot retrieval, effectively compensating for the scarcity of initial context.

Steps	Set-Rec@10	Jump (90%)	NRM
<i>Query Only</i>			
10	44.69%	–	$\mathcal{E}_{\text{base}} \cap \mathcal{E}^* = \emptyset$
<i>Additive</i>			
5+5	−3.08pp	20.3 (33.0)	−4.36pp
3+7	−4.13pp	28.3 (46.4)	−5.20pp
<i>GRAIL (Ours)</i>			
8+1+1	+1.99pp	30.1 (52.0)	+2.78pp
8+2	+1.92pp	30.2 (51.0)	+2.72pp
5+5	+0.96pp	34.4 (66.2)	+2.74pp
3+7	+0.22pp	34.2 (65.2)	+1.75pp
3+3+4	+1.32pp	34.6 (58.4)	+2.89pp
3+2+3+2	+2.00pp	30.3 (54.5)	+3.94pp
2*5	+1.80pp	32.5 (59.0)	+3.64pp
1*10	+1.48pp	32.9 (67.1)	+2.30pp

breaks down these behaviors for $K = 10$. Each strategy denotes the step-wise retrieval slice sizes (e.g., 3+7 indicates retrieving 3 assets as the base, then 7 in the next turn).

Efficiency Amplification The behavior of the Jump metric in Table 3 demonstrates a substantial expansion of the effective search horizon. Across all configurations, GRAIL successfully retrieves complementary evidence originally ranked between the 30th and 35th positions in the baseline pool (mean Jump ≈ 30 –34). This dynamic implies that sequential information subtraction allows a compressed pool of size $K = 10$ to achieve the coverage and search depth equivalent to a three-fold larger Query Only pool. Consequently, our framework offers a resource-efficient alternative that consistently improves gold evidence coverage within a restricted budget, reducing downstream context overhead.

Robustness in Noise-Heavy Environments The NRM in Table 3 evaluates framework stability when the initial pool contains zero gold evidence and is entirely polluted by distractors. Under such noise, traditional paradigms—such as additive rewriting or explicit query regeneration—suffer from error propagation; irrelevant initial documents aggressively mislead subsequent retrieval turns. In contrast, our framework utilizes projection-based residual subtraction, bypassing fragile textual rewriting. By tracking uncovered information directly within the embedding space, the model

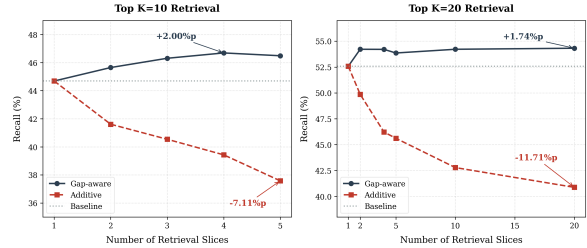


Figure 3: **Robustness of GRAIL vs. Additive models under iterative slicing.** Set-Recall(%) is plotted against the number of retrieval slices in MultimodalQA for $K = 10$ (left) and $K = 20$ (right). Although the Additive baseline exhibits strength in specific single-stage question types (Table 1), it suffers from rapid performance decay under iterative configurations due to error accumulation (see Appendix D for extended analysis).

maintains structural robustness even when the initial step is completely blind, achieving a peak robustness gain of **+3.94pp** under 3+2+3+2 strategy.

5.5 Analysis of Pre-alignment Spaces

We analyze how cross-modal alignment topologies and training regimes affect latent steering. While query-independent spaces require full fine-tuning (FT) due to coarse feature subtraction, query-dependent approaches perform optimally when frozen, as full FT disrupts pre-aligned semantic boundaries. Crucially, the *Query-evidence* alignment strikes the best balance—capturing precise local contexts while preserving pre-aligned semantic boundaries and yielding a positive Δ_{esc} . In contrast, *Query-set* alignment suffers from grain-dilution, collapsing localized precision. Consequently, we establish *Query-evidence* as our default topology. We provide full empirical results and deeper theoretical implications in Appendix C.

6 Conclusion

In this paper, we addressed Semantic Anchoring in MMQA retrieval, where conventional additive methods suffer from entity-centric redundancy. To overcome this, we introduced GRAIL, an implicit context-subtractive query rewriting mechanism operating directly in the shared latent space without error-prone textification. Moreover, our Hybrid Framework dynamically routes queries to task-specific specialists to maximize baseline synergies. Extensive evaluations on MultimodalQA confirm that GRAIL expands the effective search horizon, demonstrates robust noise-resilience, and outperforms explicit query generation baselines.

Limitations

While our proposed framework demonstrates significant efficacy and robustness in implicit latent steering for multimodal multi-hop retrieval, we acknowledge several limitations that open avenues for future work.

Fixed Step Scheduling In our iterative retrieval experiments (Section 5.4), we explored a variety of fixed partitioning strategies (e.g., 3+2+3+2, 5+5) rather than dynamically adjusting the step sizes during runtime. While this structured scheduling ensures predictable latency and bypasses the computational overhead of an online decision loop, it does not adaptively recalibrate based on the complexity of an individual query. Developing an end-to-end dynamic step controller that infers the optimal stopping criterion per hop remains an open challenge.

Lack of Generative Answer Synthesis Our framework focuses strictly on the retrieval and evidence set completion phases of the multimodal multi-hop pipeline. Unlike explicit LLM-based query generation frameworks that end-to-end synthesize final natural language answers, our model is designed as a highly parameter-efficient retrieval accelerator. While it drastically reduces context window overhead and provides clean evidence pools, integrating this implicit steering mechanism with a generative downstream reader to produce comprehensive multimodal answers is left for future engineering.

Scalability to Open-Ended Web Environments

Although our empirical evaluations comprehensively cover both standard benchmarks and deep multi-hop scenarios (extending to 3+ hops), our projection-based subtraction has primarily been verified within bounded knowledge corpora. Scalability to open-ended, web-scale retrieval environments—where the density of distractors increases exponentially and the modality drift is more severe—remains an active area of investigation.

References

Yang Bai, Christan Grant, and Daisy Zhe Wang. 2025. Ramqa: A unified framework for retrieval-augmented multi-modal question answering. In *Findings of the Association for Computational Linguistics: NAACL 2025*, pages 1061–1076.

Wenhu Chen, Hexiang Hu, Xi Chen, Pat Verga, and William Cohen. 2022. Murag: Multimodal retrieval-augmented generator for open question answering over images and text. In *Proceedings of the 2022 Conference on Empirical Methods in Natural Language Processing*, pages 5558–5570.

Jacob Devlin, Ming-Wei Chang, Kenton Lee, and Kristina Toutanova. 2019. Bert: Pre-training of deep bidirectional transformers for language understanding. In *Proceedings of the 2019 conference of the North American chapter of the association for computational linguistics: human language technologies, volume 1 (long and short papers)*, pages 4171–4186.

OpenAI Aaron Hurst, Adam Lerer, Adam P. Goucher, Adam Perelman, Aditya Ramesh, Aidan Clark, AJ Ostrow, Akila Welihinda, Alan Hayes, Alec Radford, Aleksander Mkadry, Alex Baker-Whitcomb, Alex Beutel, Alex Borzunov, Alex Carney, Alex Chow, Alexander Kirillov, Alex Nichol, Alex Paino, and 397 others. 2024. [Gpt-4o system card](#).

Gautier Izacard, Mathilde Caron, Lucas Hosseini, Sebastian Riedel, Piotr Bojanowski, Armand Joulin, and Edouard Grave. 2021. Unsupervised dense information retrieval with contrastive learning. *arXiv preprint arXiv:2112.09118*.

Vladimir Karpukhin, Barlas Oguz, Sewon Min, Patrick Lewis, Ledell Wu, Sergey Edunov, Danqi Chen, and Wen-tau Yih. 2020. Dense passage retrieval for open-domain question answering. In *Proceedings of the 2020 conference on empirical methods in natural language processing (EMNLP)*, pages 6769–6781.

Peng Qi, Xiaowen Lin, Leo Mehr, Zijian Wang, and Christopher D Manning. 2019. Answering complex open-domain questions through iterative query generation. In *Proceedings of the 2019 conference on empirical methods in natural language processing and the 9th international joint conference on natural language processing (EMNLP-IJCNLP)*, pages 2590–2602.

Alec Radford, Jong Wook Kim, Chris Hallacy, Aditya Ramesh, Gabriel Goh, Sandhini Agarwal, Girish Sastry, Amanda Askell, Pamela Mishkin, Jack Clark, and 1 others. 2021. [Learning transferable visual models from natural language supervision](#). In *International conference on machine learning*, pages 8748–8763. PmLR.

J. J. Rocchio. 1971. [Relevance feedback in information retrieval](#).

Alon Talmor, Ori Yoran, Amnon Catav, Dan Lahav, Yizhong Wang, Akari Asai, Gabriel Ilharco, Hananeh Hajishirzi, and Jonathan Berant. 2021. [Multi-modal{qa}: complex question answering over text, tables and images](#). In *International Conference on Learning Representations*.

Harsh Trivedi, Niranjan Balasubramanian, Tushar Khot, and Ashish Sabharwal. 2023. [Interleaving retrieval](#)

with chain-of-thought reasoning for knowledge-intensive multi-step questions. In *Proceedings of the 61st Annual Meeting of the Association for Computational Linguistics (Volume 1: Long Papers)*, pages 10014–10037, Toronto, Canada. Association for Computational Linguistics.

Shitao Xiao, Zheng Liu, Peitian Zhang, and Niklas Muennighoff. 2023. **C-pack: Packaged resources to advance general chinese embedding**. *Preprint*, arXiv:2309.07597.

Lee Xiong, Chenyan Xiong, Ye Li, Kwok-Fung Tang, Jialin Liu, Paul Bennett, Junaid Ahmed, and Arnold Overwijk. 2020. Approximate nearest neighbor negative contrastive learning for dense text retrieval. *arXiv preprint arXiv:2007.00808*.

Wenhan Xiong, Xiang Lorraine Li, Srinivasan Iyer, Jingfei Du, Patrick Lewis, William Yang Wang, Yashar Mehdad, Wen-tau Yih, Sebastian Riedel, Douwe Kiela, and Barlas Oğuz. 2021. **Answering complex open-domain questions with multi-hop dense retrieval**. *International Conference on Learning Representations*.

Qian Yang, Qian Chen, Wen Wang, Baotian Hu, and Min Zhang. 2023. Enhancing multi-modal multi-hop question answering via structured knowledge and unified retrieval-generation. In *Proceedings of the 31st ACM International Conference on Multimedia*, pages 5223–5234.

Ori Yoran, Alon Talmor, and Jonathan Berant. 2022. **Turning tables: Generating examples from semi-structured tables for endowing language models with reasoning skills**. In *Proceedings of the 60th Annual Meeting of the Association for Computational Linguistics (Volume 1: Long Papers)*, pages 6016–6031, Dublin, Ireland. Association for Computational Linguistics.

Zhenrui Yue, Honglei Zhuang, Aijun Bai, Kai Hui, Rolf Jagerman, Hansi Zeng, Zhen Qin, Dong Wang, Xuanhui Wang, and Michael Bendersky. 2025. Inference scaling for long-context retrieval augmented generation. In *International Conference on Learning Representations*, volume 2025, pages 72914–72938.

Joohyung Yun, Doyup Lee, and Wook-Shin Han. 2025. Lilac: Late interacting in layered component graph for open-domain multimodal multihop retrieval. In *Proceedings of the 2025 Conference on Empirical Methods in Natural Language Processing*, pages 20551–20570.

A Additional Qualitative Case Study

To further illustrate the practical mechanics of GRAIL, we provide a detailed visualization of a representative multi-hop retrieval trajectory (Figure 4).

The selected query requires comparing the urban areas of *Pontarlier* and another city depicted in an image featuring a statue and multiple

fountains(*Lons-le-Saunier*). To successfully resolve this example, the retriever faces a distinct cross-modal bottleneck: it must correctly identify the visual asset as *Lons-le-Saunier* while simultaneously retrieving the target structured table (*Principal cities of Franche-Comté*) containing the precise metrics for both cities.

When analyzing the latent space and Top-10 retrieval composition for this specific trajectory, conventional paradigms suffer severely from embedding distortion. For instance, in the **Query Only** setting, while explicitly searching for “*Pontarlier*” pulls the missing table row of *Pontarlier*, the complete absence of visual context forces the model to anchor on superficial keywords such as *fountains, statue, or cities*. This populates the top ranks with irrelevant international city images. Similarly, blindly adding the context image embedding (**Query + Context**) amplifies the modality bias; the search manifold becomes 100% dominated by image representations, completely paralyzing the model’s table retrieval capabilities.

Even with **Explicit Rewriting** (IRCoT via GPT-4o-mini), a confirmation bias emerges. Instead of recognizing that the entire structured frame—the *list of principal cities of Franche-Comté*—is missing and guiding the search toward that global layout, the LLM deduces the final answer using its internal knowledge. It then regenerates an over-confident, verbose query specifically designed to justify this early conclusion. While this predictive shortcut manages to fetch the two local target rows (*Lons-le-Saunier* at 10th and *Pontarlier* at 16th), the conversational nature of the generated query introduces unnecessary noise, still retrieving a large number of irrelevant international city images within the Top-10 ranks. More importantly, rather than recognizing the global context of the *Franche-Comté* table as the primary search target, this paradigm remains heavily entity-centric. By locking into a predicted entity instead of capturing the broader table layout, it deprives the model of any opportunity to self-correct when its internal knowledge is flawed, potentially leading to a failure in delivering accurate, evidence-based reasoning.

In contrast, our context-subtractive approach (**Query - Context**) successfully redirects the query embedding toward the missing evidence. By subtracting the visual features of the context, GRAIL eliminates the dominating image-modality bias, allowing the table modality to dominate the top ranks (70% table rows) and pulling adjacent rows

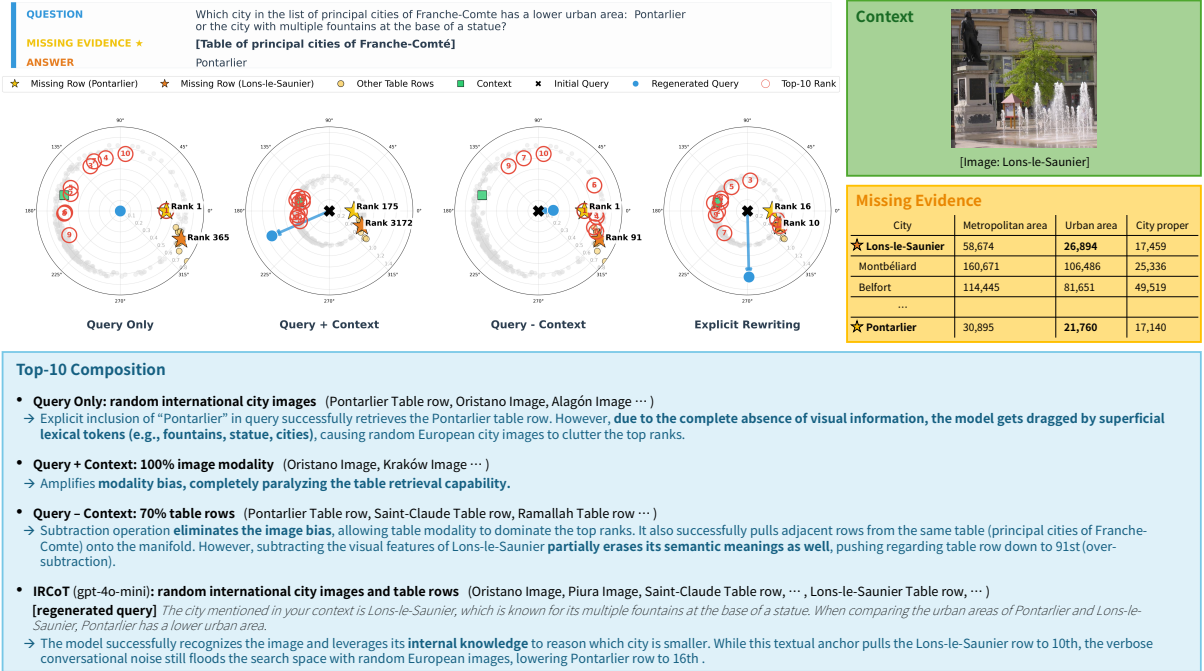


Figure 4: **Additional Case Study.** Given an image of Lons-le-Saunier, the goal is to fetch the missing table evidence (the list of principal cities of Franche-Comte) to complete the evidence set.

from the target Franche-Comté table. However, this case also uncovers a nuanced *over-subtraction* phenomenon: while the operation successfully surfaces the relevant table structure, erasing the visual features of Lons-le-Saunier partially weakens its semantic representation, meaning the missing Lons-le-Saunier row is not yet sufficiently pulled into the Top-10 ranks (remaining at the 91st rank).

Rather than a failure, we highlight the potential of an *iterative retrieval* paradigm. Since the subtractive steering successfully establishes the correct global table layout on the embedding space, these newly retrieved multi-hop evidence sets can serve as a powerful stepping stone for subsequent iterations. By leveraging this structured foundation in the next retrieval loop, the model can naturally recover the weakened local entities, progressively narrowing the semantic gap without introducing conversational or modality bias.

B Detailed Experiments Setup

B.1 Detailed MultimodalQA Statistics

Detailed statistics of the MultimodalQA benchmark (Talmor et al., 2021) splits used in this work are summarized in Table 4 and Table 5.

Table 4: Statistics of the MultimodalQA corpus.

Modality	Text	Table	Image	Total
Count	218,285	144,407	57,058	419,750

Table 5: Statistics of the MultimodalQA question type. Unique QIDs are expanded into Total Inst. via our leave-one-out approach.

Q_Type	Train	Val	Test	Total
Uni-modal	3,182	365	409	3,956
Intersect	1,069	161	149	1,379
Compare	1,317	165	159	1,641
Compose	4,964	625	600	6,189
Unique QIDs	10,532	1,316	1,317	13,165
Total Inst.	31,095	3,929	4,024	39,048

B.2 Pseudocode of Implicit Query Rewriting

Given the raw query q and the currently acquired partial evidence set \mathcal{E}_p , the procedure first aggregates existing knowledge into a context vector h_{ctx} via explicit attention routing (Eq. 6). It then dynamically computes the learnable gap gate g to modulate the intensity of the projection-based subtraction, purifying the raw query into a gap-aware representation q_{gap} (Eq. 8). Finally, the framework applies a lightweight mixing module W_{mix} to dynamically balance q_{gap} and h_{ctx} , returning the calibrated request vector h_{req} alongside the dynamically adjusted scaling temperature τ_{dyn} for end-to-end alignment calibration.

Algorithm 1 Gap-aware Subtractive Search

Require: Query q , Partial evidence set \mathcal{E}_p **Ensure:** Refined request vector h_{req} , Dynamic temperature τ_{dyn}

- 1: $V_p \leftarrow \{E(e_i) \mid e_i \in \mathcal{E}_p\}$
 - 2: $h_{\text{ctx}} \leftarrow \text{Attention}(q, V_p)$
 - 3: **if** Gap-aware (ours) **then**
 - 4: $g \leftarrow \sigma(W_{\text{gap}}[q; h_{\text{ctx}}])$
 - 5: $q_{\text{gap}} \leftarrow q - g \cdot \mathcal{F}(h_{\text{ctx}})$
 - 6: $[w_1, w_2] \leftarrow \text{Softmax}(W_{\text{mix}}[q_{\text{gap}}; h_{\text{ctx}}])$
 - 7: $h_{\text{req}} \leftarrow \text{LN}(w_1 q_{\text{gap}} + w_2 h_{\text{ctx}})$
 - 8: $\tau_{\text{dyn}} \leftarrow \exp(\log \tau_{\text{base}} + \text{MLP}([q; h_{\text{ctx}}]))$
 - 9: **else if** Additive (baseline) **then**
 - 10: $h_{\text{req}} \leftarrow \text{LN}(q + \text{LN}(h_{\text{ctx}}))$
 - 11: $\tau_{\text{dyn}} \leftarrow \tau_{\text{base}}$
 - 12: **end if**
 - 13: **return** $h_{\text{req}}, \tau_{\text{dyn}}$
-

B.3 Implementation Details

For the unified latent space, we employ BGE-large-en-v1.5 (Xiao et al., 2023) to embed questions, text passages, and table rows. Images are embedded using CLIP ViT-B/32 (Radford et al., 2021). All embeddings are projected into a shared latent space of dimension $d = 1024$. We train the retrieval model using the AdamW optimizer with a batch size of 32, 100 epochs, and a learning rate of $1e-4$. The base temperature τ_{base} is set to 0.05. All experiments are conducted on NVIDIA RTX A6000 GPUs. The selector $\Phi(q)$ is instantiated using a bert-base-uncased backbone (Devlin et al., 2019) fine-tuned independently for 3 epochs with a learning rate of $1e-5$.

C Detailed Alignment Strategies Analysis

This section extends the empirical evaluation of Section 4.1 by providing a comprehensive analysis of the interaction between cross-modal alignment topologies, training regimes (Frz vs. FT), and downstream task complexities.

C.1 Cross-Examination of Training Regimes

Table 6 presents the complete grid search across all alignment strategies and training configurations.

The empirical behavior of query-independent approaches (*None*, *Centroid*, *CLS*) further confirms that optimizing for internal evidence set cohesion alone is insufficient for multi-modal alignment. Relying solely on intra-chain similarity or static aggregation (*Centroid*, *CLS*) lacks a definitive semantic

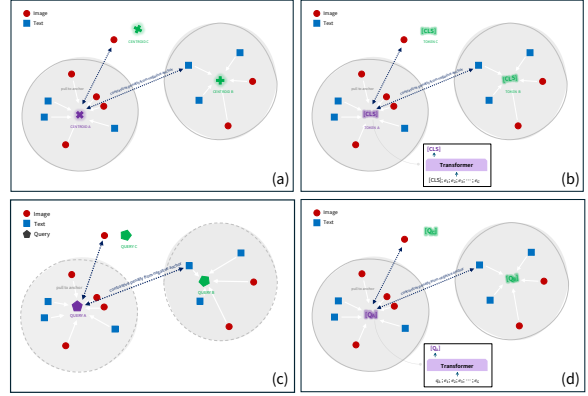


Figure 5: **Taxonomy of cross-modal semantic alignment.** Top row shows query-independent approaches: (a) Centroid-based alignment, (b) CLS-based alignment. Bottom row shows query-dependent approaches: (c) Query-evidence alignment, (d) Query-set alignment.

Table 6: **Retrieval performance of gap-aware mechanism across different alignment strategies in Multi-modalQA.** Full empirical comparison across all cross-modal topologies under both frozen and fine-tuned training regimes. (FT: full fine-tuning, Frz: frozen backbones).

Alignment		R@1	R@5	R@20	R@50	Δ_{esc}
None	Frz	0.48	10.33	25.55	31.13	-0.011
	FT	8.35	22.88	42.25	50.04	+0.043
Centroid	Frz	0.74	12.90	33.42	41.84	-0.147
	FT	5.17	19.70	37.77	44.62	-0.210
CLS	Frz	0.74	12.93	36.01	45.13	-0.162
	FT	6.11	19.67	35.00	41.94	-0.180
Query-evidence	Frz	15.68	31.15	47.85	58.34	+0.007
	FT	8.30	21.63	34.56	42.22	-0.034
Query-set	Frz	4.50	24.43	48.97	60.52	-0.136
	FT	4.40	22.47	46.65	53.35	-0.149

anchor to justify why disparate modalities should co-exist within the same evidence chain. Without a central medium to synthesize these cross-modal fragments, frozen setups (Frz) yield near-zero performance (e.g., R@1 of 0.48% for *None* and 0.74% for both *Centroid* and *CLS*), requiring full fine-tuning (FT) to forcefully warp the unconditioned representations into task-relevant boundaries.

In contrast, our query-dependent formulations introduce the query as an explicit semantic medium. Rather than blindly pushing text, tables, and images together, strategies like *Query-evidence* leverage the query to explicitly contextualize why these specific cross-modal segments belong to the same evidence chain. Consequently, when this already optimized space undergoes full fine-tuning (FT), it triggers severe overfitting and representation drift instead of further adaptation. As evidenced by the *Query-evidence* R@1 dropping drastically from

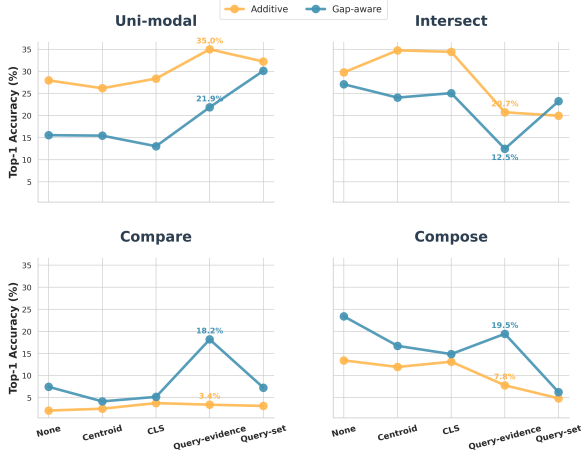


Figure 6: **Model specialization by task complexity in MultimodalQA.** Additive models excel in Uni-modal lookup, while Gap-aware models dominate reasoning-heavy tasks (Compare, Compose). This performance gap remains consistent across alignment architectures.

15.68% to 8.30% (with Δ_{esc} turning to -0.034), full parameter updates break the highly precise, cross-modal arrangements. Therefore, as established in our main experiments (Section 5.5), we evaluate each alignment style under its respective optimal training regime (FT for query-independent and Frz for query-dependent settings) to conduct a follow-up analysis.

C.2 Alignment Adaptability by Question Type

To analyze how alignment strategies interact with specific question characteristics, Figure 6 breaks down the performance across distinct question categories (Uni-modal, Intersect, Compare, Compose). The results reveal a clear architectural specialization rooted in the type of reasoning required:

- **Localized Aggregation Tasks** (Uni-modal, Intersect): The conventional Additive baseline consistently outperforms, peaking at 35.0% recall in Uni-modal queries. These tasks primarily rely on single-modality lookups or localized information aggregation where representation fusion is sufficient. In these environments, our subtractive steering introduces unnecessary geometric disruption to vectors that are already optimal for concentrated entity matching.
- **Compositional Reasoning Tasks** (Compare, Compose): Our Gap-aware mechanism dominates the baseline, achieving 18.2% accuracy in *Compare* (vs. 3.4% for Additive) and

19.5% in *Compose* (vs. 7.8% for Additive). Because these tasks demand genuine compositional cross-modal reasoning—where information across disparate modalities and distinct entities must be cross-referenced without redundancy—GRAIL successfully isolates the missing semantic fragments where additive methods fail.

By observing the distinct behavior of each alignment strategy across these tasks, we propose several hypotheses regarding how vector space constraints impact retrieval.

Specifically, for **Uni-modal** queries, the Additive baseline exhibits a sharp upward trajectory that explicitly peaks at the *Query-evidence* stage, reaching its highest accuracy of 35.0%. Since Uni-modal tasks can be resolved entirely within a single modality, the retrieval space does not require complex multi-modal bridging. In this context, *Query-evidence* provides the clean lexical-to-semantic alignment needed to guide the additive vector update straight toward the target zone within specific modality.

Conversely, for **Intersect** queries, the Additive architecture achieves its performance plateau at the query-independent *Centroid* and *CLS* stages, but experiences a significant drop down to 20.7% at the *Query-evidence* stage. We hypothesize that Intersect tasks inherently require capturing the overlapping intersection across disparate modalities. Query-independent pre-alignment naturally compacts these heterogeneous text, table, and image assets into a dense, shared cross-modal cluster beforehand, making it easy for a simple additive update to fuse the multi-modal evidence. However, because the *Query-evidence* strategy focuses strictly on mapping the query to each asset individually, it fails to bind the disparate modalities to one another. This lack of direct cross-modal cohesion isolates the assets from each other, fracturing the dense cluster structure and making localized information aggregation for Intersect queries much more difficult.

Conversely, in the **Compare** task, while query-independent methods severely degrade retrieval, the query-dependent *Query-evidence* strategy yields a powerful performance spike. This behavior indicates that comparison tasks inherently require query-centric alignment rather than inter-asset correlations. Because the target assets often share no intrinsic relationship other than being re-

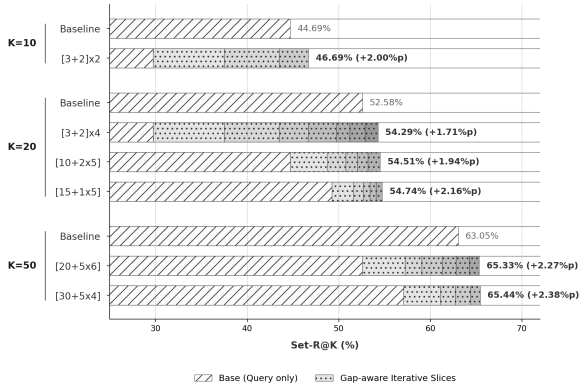


Figure 7: **Set Recall across varying pool sizes (K)**. The leftmost dashed segment represents the initial Base (Query Only) retrieval, while subsequent segments illustrate cumulative gains from the sequential execution of iterative GRAIL slices (e.g., $[3+2]*2$ denotes a 3(base)+2+3+2 step sequence, darkening chronologically). Across all pool sizes, our iterative framework consistently expands retrieval coverage, demonstrating sustained gains even as the retrieval constraints scale.

requested by the same query, forcing query-free clusters groups them by irrelevant modal or thematic similarities, making it highly counterproductive for reasoning. In contrast, the *Query-evidence* strategy successfully maps each asset directly to the query, providing the clean contrastive space needed to compare distinct entities.

Finally, the **Compose** task uncovers a unique phenomenon: the unaligned *None* setup yields the highest accuracy for the gap-aware mechanism, while among the pre-aligned alternatives, performance peaks at *Query-evidence*. This behavior likely stems from *representation collapse* during the alignment phase. Because compositional queries require assembling open-ended evidence fragments, forcing a structured alignment objective shifts the representations toward rigid cluster centers. This restriction compresses the semantic flexibility needed to link disparate pieces of evidence. While the unaligned (*None*) space preserves this flexibility intact for subtractive isolation, the item-level granularity of the *Query-evidence* configuration serves as the optimal alternative among the aligned models by minimizing global spatial distortion.

D Detailed Analysis on Iterative Retrieval

Figure 7 illustrates the overall retrieval recall across different total pool sizes ($K \in \{10, 20, 50\}$). Our gap-aware iterative strategy consistently yields ro-

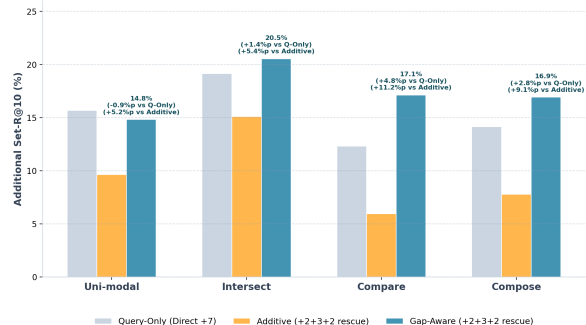


Figure 8: **Breakdown of additional retrieval gains by question type**. The bars represent the isolated increase in Set-Recall contributed exclusively by the 7 additional evidence pieces retrieved after the initial *Query Only* baseline (Base 3). Note that the baseline recall at Base 3 is omitted, plotting only the net incremental gain captured during the remaining sequential rescue steps (partitioning scheme 3+2+3+2). All values represent the percentage point (%pp) improvement, mapping the distinct behavior of the static *Query Only* baseline, the *Additive* model, and our *Gap-Aware* mechanism across the four question categories of MultimodalQA dataset.

bust gains over the baseline across all expanded budgets (+2.00%pp for Top-10, +2.16%pp for Top-20, and +2.38%pp for Top-50).

To investigate the dynamic behavior of multi-hop retrieval across distinct question categories, Figure 8 illustrates the incremental Set-Recall@10 gains achieved exclusively during the sequential rescue steps (partitioning scheme 3+2+3+2). The results show that our GRAIL consistently delivers the highest retrieval gains across all task types except Uni-modal. Particularly in the *Compare* category, GRAIL outperforms the *Query Only* baseline by 4.5pp and the *Additive* model by 11.2pp.

This stark gap stems from the *Additive* framework’s inherent vulnerability to retrieval noise. When irrelevant or noisy assets are captured in the initial retrieval phase, the additive model continuously accumulates these corrupted contexts into the updated query vector. Consequently, no matter how many iterative steps are executed, the expanded query remains heavily distorted by the embedded noise, failing to retrieve the actual missing entities. In contrast, our subtractive operator successfully shielding the query from accumulated noise and shifting the search focus toward the remaining semantic gaps.

An identical vulnerability directly accounts for the performance decay observed under iterative retrieval regimes. While the *Additive* approach is

Table 7: **Distribution of gating coefficients and mixing weights on MultimodalQA.** Values are reported as mean (standard deviation) on the MultimodalQA validation set. Across all question categories, the mixing weight w_1 consistently converges near 1.000 with near-zero variance, indicating that the framework universally prioritizes the isolated semantic gap (q_{gap}) over the existing context restoration.

Category	Gate g	Weight w_1	Weight w_2
Uni-model	0.267 (0.089)	1.000 (0.001)	0.000 (0.001)
Intersect	0.286 (0.098)	1.000 (0.000)	0.000 (0.000)
Compare	0.311 (0.082)	1.000 (0.000)	0.000 (0.000)
Compose	0.303 (0.084)	1.000 (0.001)	0.000 (0.001)
Overall	0.288 (0.091)	1.000 (0.001)	0.000 (0.001)

known to perform well when initialized with clean, partial gold evidence (Evidence Set Completion), its performance collapses in realistic setups that start from unverified *Query Only* baselines (Sequential Pool Construction). Without the guarantee of gold context, the additive fusion absorbs initial retrieval errors, whereas GRAIL yields stable, superior improvements by strictly isolating the remaining semantic gaps without amplifying noise.

E Ablation Study

To understand the inner workings of GRAIL, we analyze the behavior of the dynamic gating coefficient (g) and the mixing weights (w_1, w_2) across different question categories, followed by an ablation study removing the dynamic mixing module (W_{mix}).

Analysis on Gating and Weight Distributions

Table 7 provides a detailed statistical breakdown of the learned parameters. The dynamic gating coefficient g maintains an overall average of 0.288, with slightly higher activation in compositional cross-modal reasoning tasks such as *Compare* (0.311) and *Compose* (0.303). This confirms that the model actively modulates the intensity of the subtractive operation based on the reasoning depth required.

The learned mixing weights exhibit an extreme and highly consistent distribution: across all categories, w_1 converges directly to 1.000 with a standard deviation of ≤ 0.001 , while w_2 effectively remains at 0.000. Originally, the mixing layer W_{mix} was introduced to regularize the updated query vector, acting as a logical anchor by blending the saturated context (h_{ctx}) back to maintain reasoning continuity. However, the empirical results show that the model universally assigns near-zero weight,

allocating its full attention to the isolated semantic gap (q_{gap}). This absolute convergence indicates that the subtractive vector steering mechanism is structurally sufficient to drive the retrieval process independently, rendering the additive restoration of h_{sat} largely redundant.

Table 8: **Evidence Set Completion performance with and without dynamic mixing.** Recall metrics ($R@k$) are reported in percentages (%). Both configurations yield highly comparable results across most task categories, aligning with the weight distribution analysis where the mixing weight w_1 naturally converges near 1.000.

Category	Model	R@1	R@5	R@10	R@20	DC-Gap
Uni-model	Ours	21.00	33.94	40.91	46.72	-0.010
	w/o W_{mix}	20.91	33.44	40.83	49.05	-0.013
Intersect	Ours	14.61	30.70	38.10	46.50	-0.066
	w/o W_{mix}	14.12	31.69	39.29	47.98	-0.066
Compare	Ours	18.29	33.25	38.72	45.84	+0.046
	w/o W_{mix}	17.81	32.54	39.43	46.79	+0.041
Compose	Ours	20.31	36.51	42.79	50.00	+0.087
	w/o W_{mix}	20.08	35.81	43.41	49.77	+0.076

Table 9: Sequential Pool Construction performance comparison between GRAIL (ours) and without W_{mix} on the MultimodalQA dataset. Improvements in Set-Recall@10 and Noise-Resilience Margin (NRM) are relative to the Query Only model (44.69% Set-Rec@10). Rank Jump values and their standard deviations are formatted as mean (std.dev.).

Model	Steps	Set-Rec@10	Jump	NRM
Ours	8+1+1	+1.99pp	30.1 (40.5)	+2.78pp
w/o W_{mix}	8+1+1	+1.71pp	28.4 (38.2)	+2.50pp
Ours	5+5	+0.96pp	34.4 (51.9)	+2.74pp
w/o W_{mix}	5+5	+1.39pp	32.8 (51.1)	+3.46pp
Ours	3+7	+0.22pp	34.2 (51.9)	+1.75pp
w/o W_{mix}	3+7	+0.27pp	33.2 (51.3)	+2.03pp
Ours	3+3+4	+1.32pp	34.6 (54.8)	+2.89pp
w/o W_{mix}	3+3+4	+1.17pp	31.6 (52.5)	+2.67pp
Ours	3+2+3+2	+2.00pp	30.3 (38.7)	+3.94pp
w/o W_{mix}	3+2+3+2	+1.76pp	33.5 (46.8)	+3.66pp
Ours	1*10	+1.48pp	32.9 (43.1)	+2.30pp
w/o W_{mix}	1*10	+1.68pp	30.9 (41.4)	+2.18pp

Impact of Removing Dynamic Mixing To evaluate the necessity of the dynamic mixing module, Table 8 and Table 9 compare the full GRAIL framework against the subtraction-only variant ($w/o W_{\text{mix}}$, where $w_1 = 1$).

Consistent with our analysis on the weight distributions where w_1 naturally converges near 1.000,

both configurations yield highly comparable performance across most retrieval settings. In Evidence Set Completion task (Table 8), removing W_{mix} causes marginal fluctuations but maintains comparable performance, confirming that q_{gap} alone carries the core retrieval signal. Similarly, in Sequential Pool Construction (Table 9), the subtraction-only baseline closely tracks or occasionally matches the full model’s performance in alternate partitioning schemes like 5+5 or 3+7.

Nevertheless, because the full GRAIL framework consistently achieves the best overall performance in dense retrieval steps (e.g., yielding the highest peak of +2.00pp in the 3+2+3+2 Set-Rec@10), we retain the dynamic mixing module as our primary configuration for reporting the main results.

F Generalization on WebQA

To verify the dataset-agnostic scalability of our framework, we evaluate GRAIL on the WebQA dataset, a large-scale multimodal retrieval benchmark (Corpus statistics detailed in Table 10 and Table 11). Distinct from MultimodalQA requiring complex cross-modal fusion per query, WebQA serves as a unified multimodal corpus consisting of separate text and image modalities, where each question focuses on retrieving multiple images or multiple text snippets scattered across the heterogeneous collection.

Table 10: Statistics of the WebQA corpus.

Modality	Text	Image	Total
Count	666,998	389,740	1,056,738

First, the learned parameter distributions on WebQA (Table 12) tightly echo our findings on MultimodalQA: the dynamic mixing weight w_1 universally converges to 1.000 with near-zero standard deviations (≤ 0.005) across all query types. This absolute convergence reinforces our core geometric hypothesis that the isolated semantic gap (q_{gap}) dominates the retrieval space independently. Furthermore, the pre-alignment evaluation (Table 13) confirms that the frozen *Query-evidence* configuration serves as the optimal topological prerequisite, yielding a powerful peak performance (e.g., 43.15% R@5 vs. 16.26% for None).

Interestingly, the category-wise comparison between Additive and GRAIL (Table 14) reveals a clear performance trade-off. As previously observed in the MultimodalQA dataset experiments,

Table 11: Statistics of the WebQA question type.

Question Type	Train	Val	Test	Total
text	32,827	4,153	4,169	41,149
number	264	60	36	360
YesNo	6,848	790	844	8,482
choose	4,590	608	516	5,714
color	834	70	108	1,012
shape	136	6	14	156
Others	2,514	316	322	3,152
Total Inst.	48,013	6,003	6,009	60,025

Table 12: **Distribution of gating coefficients and mixing weights on WebQA.** Values are reported as mean (standard deviation). Similar to MultimodalQA, w_1 consistently converges to 1.000 across all query types with near-zero variance, isolating the subtractive gap.

Category	Gate g	Weight w_1	Weight w_2
text	0.186 (0.070)	1.000 (0.001)	0.000 (0.001)
number	0.081 (0.085)	1.000 (0.000)	0.000 (0.000)
YesNo	0.075 (0.078)	1.000 (0.002)	0.000 (0.002)
choose	0.139 (0.107)	1.000 (0.001)	0.000 (0.001)
color	0.092 (0.097)	1.000 (0.000)	0.000 (0.000)
shape	0.096 (0.088)	1.000 (0.000)	0.000 (0.000)
Others	0.065 (0.067)	1.000 (0.005)	0.000 (0.005)

the *Additive* model shows strength when retrieving evidence within the same, single modality. Because individual queries in WebQA focus on finding multiple assets from the exact same modality (either only text snippets or only images), this dataset is also likely to favor the *Additive* baseline. This allows Additive to perform better in minor attribute tasks such as *Number*, *YesNo*, and *Shape*.

However, GRAIL shows a massive reversal when given enough training data to learn this non-cross-modal environment. In data-rich categories like *Text* and *Others* (see Table 11), where the model has sufficient examples to optimize its vector steering layers, GRAIL heavily outperforms the baseline—boosting the *Text* category by a massive **26.0%pp** in R@1. Conversely, in minor categories like *Number* and *Shape*, the severe data scarcity makes it difficult for GRAIL to train its dynamic gating parameters, leaving them reliant on Additive’s simple token accumulation.

Importantly, even when raw recall fluctuates due to sample scarcity, a closer inspection of the set completion metric (Δ_{esc}) reveals that the *Additive* framework suffers from systemic collapse, yielding negative margins (ranging from -0.134 to -0.229) across every single category. In contrast, GRAIL consistently maintains positive Δ_{esc} values without exception, proving its robust precision.

This empirical complementarity confirms that

Table 13: **Retrieval performance of gap-aware mechanism across different alignment strategies in WebQA.** R@K metrics are reported in percentages (%). Full empirical comparison across all cross-modal topologies under both frozen and fine-tuned training regimes. (FT: full fine-tuning, Frz: frozen backbones). Mapping individual assets directly to the query via frozen *Query-evidence* serves as the optimal topological setting.

Alignment		R@1	R@5	R@20	R@50	Δ_{esc}
None	Frz	0.00	16.26	33.72	43.96	-0.157
	FT	0.00	16.67	33.83	44.28	-0.162
Centroid	Frz	0.00	15.14	31.65	42.13	-0.276
	FT	0.00	15.09	31.62	41.65	-0.265
CLS	Frz	0.02	5.21	12.11	18.29	-0.178
	FT	0.03	5.48	11.76	17.31	-0.333
Query-evidence	Frz	25.60	43.15	57.14	64.77	+0.036
	FT	0.00	17.29	35.82	47.26	-0.465
Query-set	Frz	11.21	37.66	56.27	65.45	-0.127
	FT	0.00	17.66	35.22	46.94	-0.454

Table 14: **Retrieval performance across question types in WebQA.** Comparison between the Additive baseline and GRAIL subject to q_type.

Type	Method	R@1	R@5	R@10	R@20	Δ_{esc}
Text	Additive	11.97	49.87	63.64	74.14	-0.228
	GRAIL	37.95	60.68	69.30	75.85	+0.043
Number	Additive	16.67	30.00	38.33	40.00	-0.141
	GRAIL	5.00	11.67	16.67	16.67	+0.014
YesNo	Additive	3.42	12.78	18.10	25.57	-0.205
	GRAIL	2.41	6.71	10.51	16.58	+0.014
Choose	Additive	1.64	4.77	7.57	10.86	-0.229
	GRAIL	1.64	5.10	8.06	12.83	+0.032
Color	Additive	0.00	10.00	21.43	24.29	-0.210
	GRAIL	1.43	8.57	8.57	17.14	+0.020
Shape	Additive	16.67	66.67	66.67	83.33	-0.134
	GRAIL	0.00	16.67	33.33	66.67	+0.020
Others	Additive	4.43	12.97	18.67	23.73	-0.203
	GRAIL	2.85	8.54	12.03	18.67	+0.012

no single vector operator universally dominates all retrieval tasks, directly justifying our **Hybrid framework** guided by a lightweight question type selector (99.47% accuracy, 0.99 F1-score). As illustrated in Figure 9, this hybrid architecture dynamically dispatches data-rich reasoning queries to GRAIL while routing localized attribute tasks to the Additive specialist, capturing a unified “best-of-both-worlds” performance.

Finally, Sequential Pool Construction trials in WebQA (Table 15) demonstrate GRAIL’s superior noise-resilience and structural robustness over iterative steps. Admittedly, GRAIL here does not universally achieve positive gains across all partition schemes, showing slight performance drops in coarse schedules such as 5+5 (-0.22pp) and 3+7 (-0.53pp).

This phenomenon is intertwined with WebQA’s

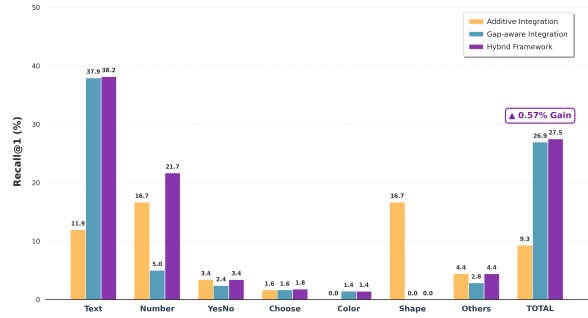


Figure 9: **Hybrid framework leveraging complementary specialists in WebQA.** By dynamically routing each query to the optimal specialist, our Hybrid framework achieves a “best-of-both-worlds” performance. (+195.7% micro avg. gain over Additive)

Table 15: **Granular efficiency under various step configurations ($K = 10$) in WebQA.** Relative improvements are measured related to Query Only baseline. GRAIL maintains robust, positive margins across granular partition schedules, whereas the Additive framework suffers severe performance degradation.

Steps	Set-Rec@10	Jump	NRM
Query Only			
10	51.06%	-	-
Additive			
5+5	-1.50pp	25.3	-2.06pp
3+7	-2.53pp	31.9	-3.61pp
GRAIL (Ours)			
8+1+1	+0.25pp	15.4	+0.59pp
8+2	+0.23pp	16.4	+0.69pp
5+5	-0.22pp	16.1	-0.20pp
3+7	-0.53pp	15.5	+0.00pp
4+3+3	+0.27pp	16.4	+0.46pp
3+2+3+2	+0.10pp	16.2	+0.45pp
2*5	-0.02pp	16.7	-0.13pp
1*10	+0.05pp	17.0	-0.11pp

evidence distribution, where most queries need roughly two gold assets, and the strong *Query Only* baseline typically captures at least one gold item in the top- K retrieval pool. However, GRAIL exhibits significantly higher mitigation against this noise-heavy environment compared to the *Additive* framework, which completely collapses as it continuously absorbs the corrupted contexts. By explicitly canceling out the first captured gold item, GRAIL successfully shields the search vector from catastrophic drift, enabling positive recovery when steps are executed with higher granularity (e.g., reaching **+0.27pp** Set-Recall and **+0.46pp** NRM in 4+3+3).

G Inference Cost Comparison

Based on the efficiency profiles in Table 16, we evaluate the computational and financial viability

Table 16: **Inference efficiency and operational cost comparison.** All configurations utilize precomputed asset embeddings, requiring zero evidence encoder passes during inference. GRAIL completely eliminates the autoregressive LLM inference loop required by explicit query generation baselines, achieving millisecond-level latency and zero API cost while maintaining robustness to retrieval noise.

Model/ Cost Dimension	Query Only	Additive	GRAIL (ours)	No-Ctx	IRCoT	Ans-Aug
LLM API Calls (per Q)	0	0	0	1	1	1
Question Encoder Passes	1	1	1	1	1	1
Active Parameter Scale	~335M	~335M	~335M+1.3M	— ~335M + LLM (7B–100B) —		
Trainable Parameters	3.68M	3.68M	5.00M (3.68M + 1.32M)	— 3.68M (Shared Alignment Base) [‡] —		
Avg. Input Tokens	0	0	0	≈ 100	≈ 776	≈ 776
Avg. Output Tokens	0	0	0	≈ 15	35.6	42.6
Avg. Latency (per Q)	2–5 ms	2–5 ms	3–6 ms	0.6–1.0 s	1.1–1.6 s	1.2–1.8 s
Relative Throughput	~400×	~400×	~350×	1.8×	1.0× (Base)	0.9×
API Cost (per 1K Qs) [†]	\$0.00	\$0.00	\$0.00	\$0.024 / \$0.40	\$0.138 / \$2.30	\$0.142 / \$2.37
Vulnerability to Noise	N/A	High	Low	N/A	Moderate	Moderate

[†] Costs are formatted as GPT-4o-mini / GPT-4o tiers. [‡] LLM-based models utilize the frozen 3.68M parameters from our optimized alignment phase to perform the initial dense asset retrieval.

of GRAIL against explicit query regeneration via LLMs.

ployment framework.

Latency and Throughput Disparity Explicit LLM query regeneration introduces severe inference bottlenecks due to its autoregressive generation. As reported in Table 16, *IRCoT* and *Answer-Augmented Retrieval* require an average of 1.1–1.6 and 1.2–1.8 seconds per question, heavily burdened by processing ≈776 input tokens and generating up to 42.6 output tokens per step. In contrast, GRAIL completely bypasses the LLM inference loop during retrieval. By executing context-subtractive query steering via a lightweight gating mechanism, our framework achieves a near-instantaneous latency of just 3–6 ms per question. This translates to a ~350× **throughput advantage**, enabling real-time, large-scale multimodal retrieval.

Financial and API Cost Analysis The operational expenses further highlight the scalability of GRAIL. LLM-based query regeneration incurs substantial commercial API costs that scale linearly with token volume. For instance, evaluating 1K questions under *IRCoT* costs up to \$2.30 via premium tiers like GPT-4o, and remains a noticeable overhead (\$0.138) even with lightweight alternatives like GPT-4o-mini. Conversely, GRAIL operates at a strict **\$0.00 API cost** by relying solely on local bi-encoder operations over precomputed embeddings. By replacing explicit text-based query generation with vector subtraction, our method eliminates financial dependencies on external commercial APIs, providing a fully self-contained de-